

## Influence of phase diffusion on spontaneous oscillations in driven optical systems

M. Brambilla, L. A. Lugiato, and G. Strini

*Dipartimento di Fisica dell'Università degli Studi di Milano, via Celoria 16, I-20133 Milano, Italy*

L. M. Narducci

*Physics Department, Drexel University, Philadelphia, Pennsylvania 19104*

(Received 29 January 1986)

We analyze how phase noise degrades or, sometimes, even creates temporal structures in the laser with an injected signal and in optical bistability. In the case of a laser with an injected signal, the influence of the phase fluctuations of the driving field is considerably larger than what one might expect on the basis of intuitive arguments.

### I. INTRODUCTION

Driven optical systems such as the laser with an injected signal<sup>1</sup> (LIS) and optical bistability<sup>2</sup> (OB) can display a rich variety of dynamical behaviors, from simple period-doubling bifurcations to the formation of more complicated structures, including dynamical chaos. In the study of these phenomena the external driving field has often been assumed to be in a coherent Glauber state<sup>3,4</sup> with a well-defined phase which, in turn, sets a reference for the output field. It is well known, on the other hand, that the phase of the incident field, or equivalently its frequency, is subject to random disturbances that can be described with the help of a phase-diffusion model.<sup>5</sup>

The aim of this contribution is to analyze the effect of phase diffusion on selected temporal structures that emerge as a result of instabilities in the LIS and OB systems. Hence, this work falls within the general heading of noise effects in nonlinear dynamical systems. Earlier treatments of this problem<sup>6</sup> have dealt with the progressive degradation of periodic temporal structures from increasing levels of noise, and with the overlap of external noise and deterministic chaos. We are not aware, instead, of studies that have focused specifically on the effect of phase noise. Our analysis should be valuable especially in connection with the recent experimental observations of instabilities and self-pulsing in OB (Ref. 7) and in the LIS.<sup>8,9</sup>

It is intuitively reasonable to expect that the influence of phase noise should become appreciable only when the coherence time of the input radiation becomes comparable to or even shorter than the period of the deterministic oscillations. We find instead that some temporal structures in the laser with an injected signal are far more sensitive to phase noise than this argument would lead us to believe, in the sense that the output signals develop a strong degradation even when the coherence time of the incident light is much longer than the duration of a single oscillation. In OB, instead, the influence of phase fluctuations is less pronounced, at least for the type of pulsing solutions considered in this paper.

An interesting result concerns the appearance of noise-induced oscillations even for parameter values such that

the deterministic theory predicts a stable stationary state; this type of output modulation is reminiscent of deterministic period-1 solutions, apart from the expected irregularities. Thus in this case, noise does not destroy but actually aids the development of temporal structures.

Our interest in this paper resides with the phase fluctuations of the injected field so that effects that arise from spontaneous emission or jitter in the cavity length are ignored. An earlier contribution by Chow, Scully, and Van Stryland<sup>10</sup> analyzed the role of intrinsic quantum and thermal noise in a laser with an injected signal that operates in a stationary regime. This work accounted also for the finite linewidth of the external field. In our treatment, spontaneous emission and cavity-length fluctuations can be included by adding suitable Langevin noise terms to the right-hand side of Eqs. (1). However, the analysis of this extended model is left for future work.

Spontaneous emission is certainly negligible in OB, and in most lasers the linewidth effects are overshadowed by cavity-length fluctuations. Thus in the present paper, we assume that the driven system (LIS or OB) is sufficiently well stabilized so that the main source of phase noise is the external field, and we focus on the analysis of the limitations imposed on the observation of temporal structures that arise from the finite coherence time of the driven laser.

### II. DESCRIPTION OF THE MODEL

We consider a homogeneously broadened, single-mode ring laser driven by an injected field. We label with  $\omega_A$  the center of the atomic line, with  $\omega_0$  the input carrier frequency, and with  $\omega_C$  the cavity resonance that lies nearest to  $\omega_0$ . The deterministic equations of motion are<sup>11</sup> the following:

$$\frac{dx}{d\tau} = -\bar{\kappa}(i\theta x + x - ye^{i\phi} + 2Cp), \quad (1a)$$

$$\frac{dp}{d\tau} = xD - (1 + i\Delta)p, \quad (1b)$$

$$\frac{dD}{d\tau} = -\gamma_1 \left[ \frac{1}{2}(xp^* + x^*p) + D + 1 \right], \quad (1c)$$

where  $\phi$  is the phase of the incident field and  $y$  is the amplitude normalized to the square root of the saturation intensity;  $x$  is the complex normalized amplitude of the output field;  $p$  and  $D$  are the scaled atomic polarization and population difference, respectively;  $C$  is the pump parameter. The time  $\tau = \gamma_{\perp} t$  is measured in units of the inverse atomic linewidth  $\gamma_{\perp}$ ;  $\bar{\kappa} = \kappa / \gamma_{\perp}$  is the scaled cavity linewidth, and  $\tilde{\gamma} = \gamma_{\parallel} / \gamma_{\perp}$  is the ratio between the longitudinal ( $\gamma_{\parallel}$ ) and transverse ( $\gamma_{\perp}$ ) relaxation rates;  $\Delta = (\omega_A - \omega_0) / \gamma_{\perp}$  is the atomic detuning parameter, and  $\theta = (\omega_C - \omega_0) / \kappa$  is the cavity mistuning parameter.

In this paper we focus on parameter values for which the deterministic behavior has already been studied extensively;<sup>12</sup> they are  $C = 20$ ,  $\Delta = 1$ ,  $\theta = 2$ ,  $\bar{\kappa} = 0.5$ , and  $\tilde{\gamma} = 0.05$ . The unstable range of the variable  $y$  is  $0 \leq y \leq y_M$  with  $y_M \simeq 20$ . For small values of  $y$  the system exhibits regular oscillations with a period of about  $2\pi$  units of time, corresponding to the beat note between the frequencies  $\omega_A = \omega_C$  and  $\omega_0$  [Fig. 1(a)]. Near the injection-locking threshold  $y = y_M$  the system displays period-1 oscillations with a period of about 4 units of time [Fig. 1(c)]. On decreasing the strength of the driving field, one finds a cascade of period-doubling bifurcations that eventually leads to chaotic behavior [Figs. 1(e) and 1(g)]. Additional details on the dynamic response of the LIS for these operating parameters can be found in Ref. 12.

If we replace the equilibrium population value  $+1$  with  $-1$  in Eq. (1c), we recover the mean-field model of optical bistability, with  $C$  playing the role of the bistability parameter.<sup>13,14</sup> This model predicts the occurrence of an instability that leads to regular oscillations of the transmitted intensity; in the range  $C \leq 150$ , in particular, the unstable behavior is favored by detuning and mistuning parameters having opposite signs. Pulsations of this type have been seen experimentally with a beam of atomic sodium.<sup>7</sup>

We now introduce phase noise into this model by assuming that the phase  $\phi$  of the input field is a stochastic variable undergoing a diffusion process.<sup>5</sup> The inverse of the diffusion constant is the coherence time  $\tau_c$  of the incident driving field; note that  $\tau_c$  is also measured in units of the inverse atomic linewidth  $\gamma_{\perp}^{-1} = T_2$ . Our numerical simulation of the phase-diffusion process is based on the iterative process

$$\phi(t_0 + \delta t) = \phi(t_0) + \delta\phi, \quad (2)$$

where  $\phi(t_0)$  is the phase of the incident field at some time  $t_0$  and  $\delta\phi$  is a Gaussian random variable with zero mean and a standard deviation selected in such a way as to fit the required coherence time of the incident light.

### III. NUMERICAL RESULTS FOR THE LASER WITH AN INJECTED SIGNAL

The following results are based on the numerical evaluation of very long-time series, their power spectra, and Poincaré sections. For  $y = 5$ , the distortion of the deterministic oscillations is appreciable only when  $\tau_c$  becomes comparable to the pulsation period, in qualitative agreement with the argument advanced in the Introduc-

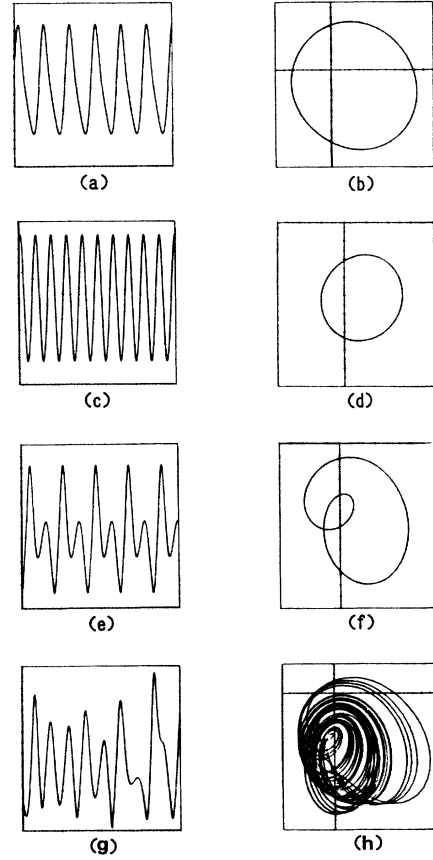


FIG. 1. (a), (c), (e), and (g) show the long-term deterministic evolution of the mod  $|x|$  of the output field for a few values of the input field  $y$ . The horizontal time scale is 40 units of  $\tau$  in all cases. The vertical scales are (a)  $4 \leq |x| \leq 11$ ; (c)  $4 \leq |x| \leq 10$ ; (e)  $0 \leq |x| \leq 14$ ; (g)  $0 \leq |x| \leq 15$ , respectively. (b), (d), (f), and (h) show the projections of the phase-space trajectory onto the plane  $x_1 = \text{Re}x$ ,  $x_2 = \text{Im}x$ ; (a) and (b) correspond to  $y = 5$ ; (c) and (d) to  $y = 18$ ; (e) and (f) to  $y = 14$ ; (g) and (h) correspond to chaotic oscillations for  $y = 12.4$ .

tion [Fig. 2(a)]. The effects induced by the phase-diffusion process are especially evident from the Poincaré maps [Figs. 2(b)–2(d)] which have been constructed, as all the other maps shown in this paper, from sequences of 160 000 time steps. Each point in the plane  $x_1 = \text{Re}x$ ,  $x_2 = \text{Im}x$  corresponds to the crossing of the phase-space trajectory with a preselected plane  $D = D_0$  (in this case  $D_0 = -0.032$ ).

For  $y = 18$ , the deterministic solution is strongly deformed even for  $\tau_c$  as large as 61.7 [Fig. 3(a)]; note that in this case the coherence time is 15 times longer than the period of a single oscillation. Clearly, the effect of phase diffusion is much stronger than in the case  $y = 5$ , as we can see by direct comparison of the Poincaré maps shown in Figs. 3(b)–3(d) and Figs. 2(b)–2(d). Figures 3(e) and 3(f) show 2 power spectra for different values of  $\tau_c$ ; note that all the spectra shown in this paper are based on the Fourier transform of  $x_1 = \text{Re}x$  and are displayed on a linear scale.

The larger sensitivity to noise for  $y = 18$  can be traced, in part, to a geometrical effect. The projection of the phase-space trajectory onto the plane  $(x_1, x_2)$  for  $y = 5$  is a

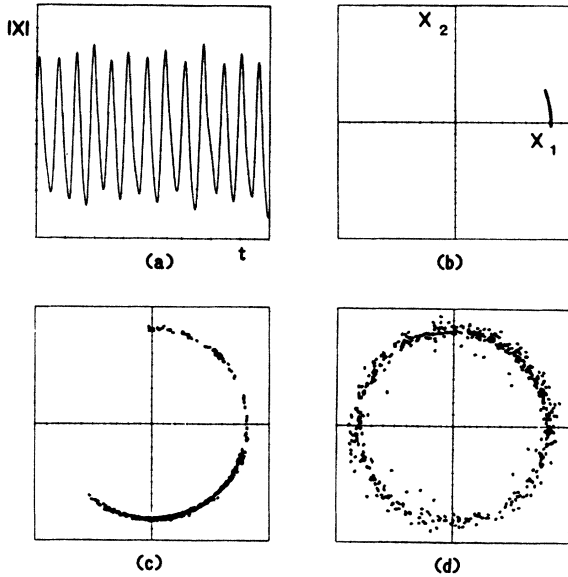


FIG. 2. Effect of phase noise for  $y=5$ . (a) Time evolution of  $|x|$  for  $\tau_c=5.56$  over 80 units of  $\tau$  (horizontal scale) and for  $2 \leq |x| \leq 12$  (vertical scale); (b), (c), and (d) show Poincaré maps for  $\tau_c=6.17 \times 10^3$ ,  $\tau_c=61.7$ , and  $\tau_c=5.56$ , respectively. The maps are plotted over the ranges  $-12 \leq x_1 \leq 12$  and  $-12 \leq x_2 \leq 12$ .

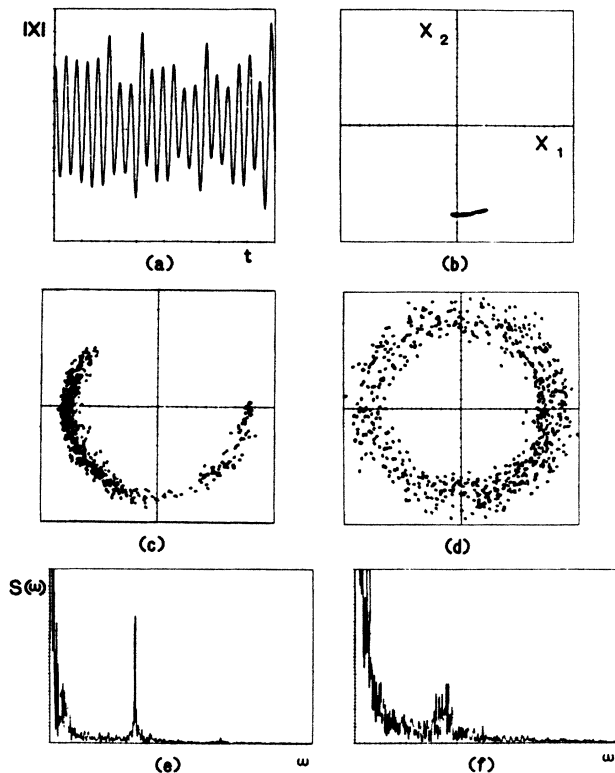


FIG. 3. Effect of phase noise for  $y=18$ . (a) Time evolution of  $|x|$  for  $\tau_c=61.7$  over 80 units of  $\tau$  (horizontal scale) and for  $2 \leq |x| \leq 12$  (vertical scale); (b), (c), and (d) show Poincaré maps for  $\tau_c=6.17 \times 10^3$ ,  $\tau_c=61.7$ , and  $\tau_c=5.56$ , respectively. The maps are plotted over the ranges  $-12 \leq x_1 \leq 12$  and  $-12 \leq x_2 \leq 12$ . (e) and (f) power spectrum  $S(\omega)$  for  $\tau_c=61.7$  and  $\tau_c=5.56$ , respectively. The frequency axis (in units of  $\gamma_1$ ) ranges from 0–314.

deformed circle surrounding the origin of the phase plane [Fig. 1(b)]. Because a transformation of the type  $\phi \Rightarrow \phi + \delta\phi$  only causes a rotation of the trajectory by a phase angle  $\delta\phi$  (or, more precisely, induces a transformation of the type  $x \Rightarrow xe^{i\delta\phi}$ ,  $p \Rightarrow pe^{i\delta\phi}$  in the output field and polarization), a circular trajectory around the origin would be entirely unaffected by the phase fluctuation. Thus for  $y=5$ , the phase-induced perturbations are rather small, while for  $y=18$  they are considerably larger; in fact, in the latter case, the phase-space trajectory, whose center is well removed from the origin of the  $(x_1, x_2)$  plane, is much more sensitive to phase changes.

For  $y=14$ , the period-2 deterministic evolution begins to be affected by the phase noise even in a situation where  $\tau_c=6.17 \times 10^3$  [Fig. 4(a)]; for  $\tau_c=61.7$  the period-2 structure is practically unrecognizable [Fig. 4(b)]. This is confirmed by the corresponding Poincaré maps [Figs. 4(c) and 4(d)] and by the power spectra [Figs. 4(e) and 4(f)].

Figure 5(a) shows a Poincaré map in the presence of deterministic chaos. This structure, which is already blurred for  $\tau_c=6.17 \times 10^3$  [Fig. 5(b)] disappears completely for  $\tau_c=61.7$  [Fig. 5(c)]. On comparing Figs. 5(d)–5(f) we see that for  $\tau_c=5.56$  the spectrum is dominated by

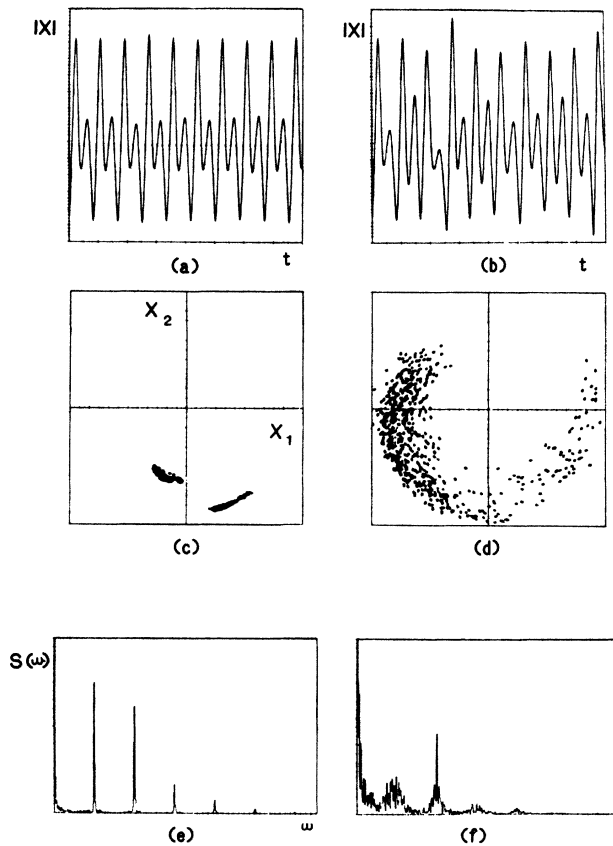


FIG. 4. Effect of phase noise for  $y=14$ . (a) Time evolution of  $|x|$  for  $\tau_c=6.17 \times 10^3$  and  $61.7$ , respectively, over 80 units of  $\tau$  (horizontal scale) and for  $0 \leq |x| \leq 14$  (vertical scale); (c) and (d) show Poincaré maps for  $\tau_c=6.17 \times 10^3$ , and  $61.7$ , respectively, (e) and (f) show power spectrum  $S(\omega)$  for  $\tau_c=6.17 \times 10^3$  and  $61.7$ , respectively. The frequency axis (in units of  $\gamma_1$ ) ranges from 0–314.

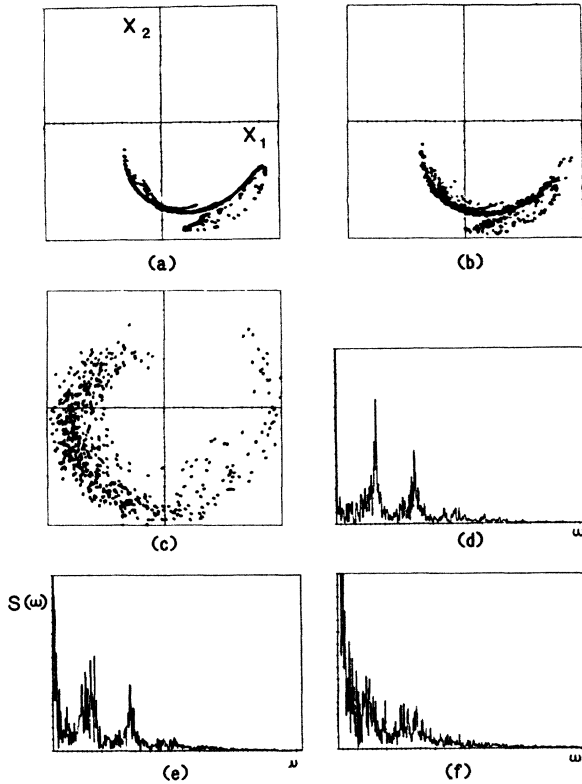


FIG. 5. Effect of phase noise for  $y=12.4$ ; (a), (b) and (c) show Poincaré maps for  $\tau_c = \infty$ ,  $6.17 \times 10^3$ , and  $61.7$ , respectively; (d), (e), and (f) show power spectrum for  $\tau_c = \infty$ ,  $61.7$ , and  $5.56$ , respectively. The frequency axis (in units of  $\gamma_1$ ) ranges from 0–314.

stochastic noise of the  $1/f$  type.

Of special interest is the problem of the correlation between the phases of the input and output fields ( $\phi_{in}$  and  $\phi_{out}$ , respectively). Plots of the output as a function of the input are shown in Fig. 6 using computer runs involving 160 000 temporal iterations. For  $y=5$  the output phase follows the input phase very closely [Fig. 6(a)]. For  $y=18$  the correlation is weaker [Fig. 6(b)], but it increases again when the coherence time becomes as small as 5.56.

For  $y=14$  and  $\tau_c=6.17 \times 10^3$  [Fig. 6(c)], the plot exhibits two distinct regions resulting from the period-2 character of the oscillations [Fig. 6(c)]; this structure disappears for  $\tau_c=6.17$  as shown in Fig. 6(d). However, the correlation between the input and output phases increases as  $\tau_c$  decreases, at least over the range of coherence times explored in these runs ( $\tau_c > 5$ ). In the chaotic case, when the coherence time is sufficiently long, the output phase is essentially uncorrelated from the input phase, as expected [Fig. 6(e)]; nevertheless, a decrease in  $\tau_c$  brings about an increase of the degree of correlation until, for  $\tau_c=5.56$ , the irregular behavior can be ascribed almost entirely to the random phase fluctuations of the input field [Fig. 6(f)].

We consider, finally, the case  $y=30$  in the presence of phase noise [Fig. 7(a)] where the stationary state is stable according to the deterministic model. Figure 7(b) has been constructed by marking a point in the plane  $(x_1, x_2)$

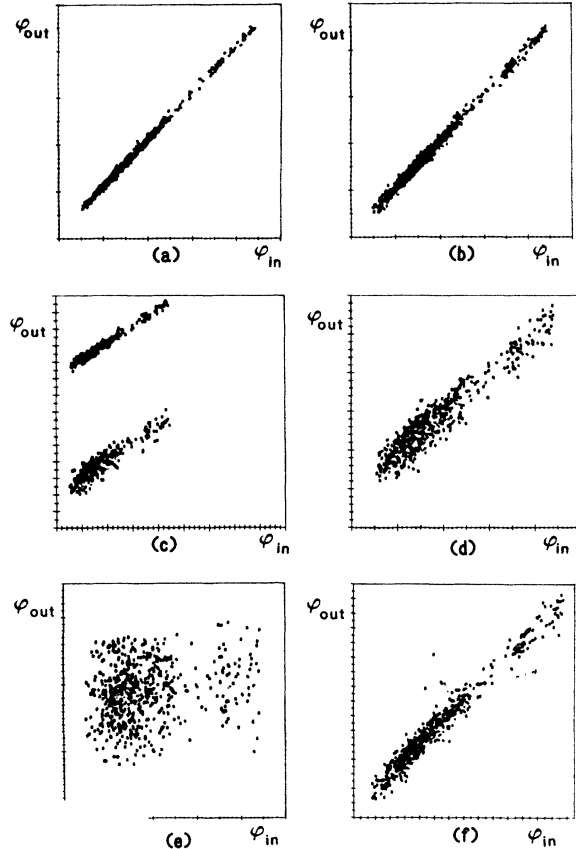


FIG. 6. The phase of the output field is plotted as a function of the phase of the input field for (a)  $y=5$ ,  $\tau_c=6.17 \times 10^3$ , (b)  $y=18$ ,  $\tau_c=6.17 \times 10^3$ , (c)  $y=14$ ,  $\tau_c=6.17 \times 10^3$ , (d)  $y=14$ ,  $\tau_c=6.17$ , (e)  $y=12.4$ ,  $\tau_c=6.17 \times 10^3$ , (f)  $y=12.4$ ,  $\tau_c=5.56$ .

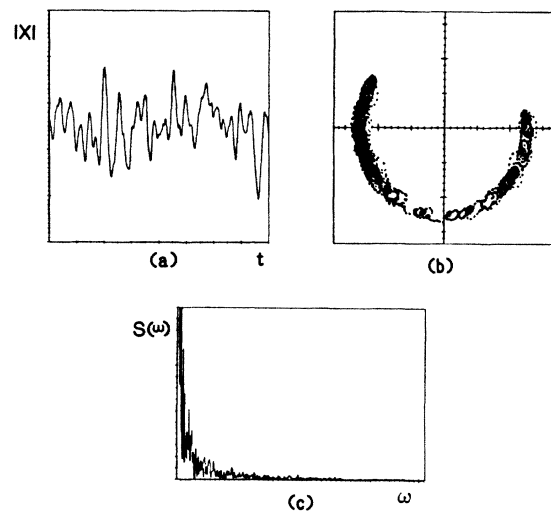


FIG. 7. Effect of phase noise for  $y=30$   $\tau_c=61.7$ ; (a) long-term time evolution of the modulus  $|x|$  of the output field over 80 units of  $\tau$  (horizontal scale) and for  $10 \leq |x| \leq 15$  (vertical scale); (b) phase-space diagram, (c) power spectrum. The frequency axis (in units of  $\gamma_1$ ) ranges from 0–314.

at intervals of 25 temporal iterations. This figure shows a remarkable similarity to the Poincaré map in the period-1 regime for  $y = 18$  and the same value of  $\tau_c$  [see Fig. 3(c)]. The temporal evolution, however, is much more erratic, as we see by comparing Figs. 7(a) and 3(a), while the power spectrum [Fig. 7(c)] does not show any structure which is evident, instead, in Fig. 3(e).

#### IV. NUMERICAL RESULTS FOR OPTICAL BISTABILITY

We study OB using the parameters  $C = 100$ ,  $\Delta = 0$ ,  $\theta = -9$ ,  $\bar{\kappa} = 0.3$ , and  $\bar{\gamma} = 1.6$ ; in this case the unstable domain corresponds to  $61.9 < y < 87.5$ . We consider two values of  $\tau_c$ ; the first,  $\tau_c = 538$ , is meant to simulate the linewidth of the driving laser field in the experiments of Ref. 7; the second,  $\tau_c = 61.7$ , is introduced to compare the response of OB with that of the LIS.

For  $y = 80$ , the period of the deterministic oscillations is about 2 units of time. The influence of phase noise is quite small for  $\tau_c = 538$  as we see in Fig. 8(a); for  $\tau_c = 61.7$  it is still considerably smaller than in the corresponding case of the laser with an injected signal [compare Figs. 8(b) and 3(a)]. Here, qualitatively, the sensitivity to noise is about the same as observed in the small- $y$  range of the LIS (e.g.,  $y = 5$ ), in spite of the fact that the projection of the phase-space trajectory on the  $(x_1, x_2)$  plane is centered away from the origin.

For  $y = 105$ , the deterministic theory predicts a stable stationary state. As shown in Figs. 8(c) and 8(d), and just as noted with the LIS, the injection of noise produces an irregular oscillatory behavior in the output signal. The presence of these oscillations may be an obstacle in attempting a quantitative comparison between the experimental instability thresholds and their theoretical counterparts.

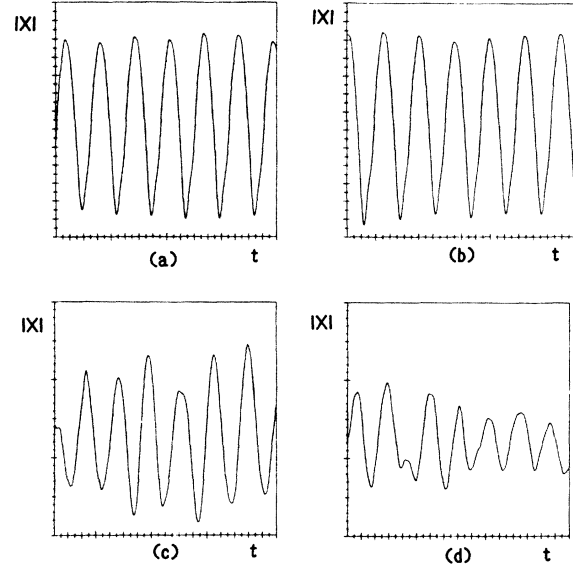


FIG. 8. Optical bistability. Snapshots of the long-time evolution for (a)  $y = 80$ ,  $\tau_c = 538$ , (b)  $y = 80$ ,  $\tau_c = 61.7$ , (c) and (d)  $y = 105$ ,  $\tau_c = 538$ . The time scale covers 16 units of  $\tau$ . The vertical scale for (a) and (b) is  $3 \leq |x| \leq 16$ , and for (c) and (d) is  $10 \leq |x| \leq 13$ .

#### ACKNOWLEDGMENTS

We are indebted to N. B. Abraham for very useful suggestions and to R. J. Horowicz for his help in preparing the numerical code. This research was carried out in the framework of an operation launched by the Commission of the European Communities under the experimental phase of the Stimulation Action. This work was supported by a grant from the Italian National Research Council (Consiglio Nazionale delle Ricerche) and by a contract with the U. S. Army Research Office (Durham, N. C.).

<sup>1</sup>See, for example, *Instabilities in Active Optical Media*, edited by N. B. Abraham, L. A. Lugiato, and L. M. Narducci [J. Opt. Soc. Am. B 2, January (1985)];  
<sup>2</sup>See, for example, *Optical Bistability 2*, edited by C. M. Bowden, H. M. Gibbs, and S. L. McCall (Plenum, New York, 1984); see also H. M. Gibbs, *Optical Bistability: Controlling Light with Light* (Academic, New York, 1985).  
<sup>3</sup>R. J. Glauber, Phys. Rev. 130, 2529 (1963).  
<sup>4</sup>R. J. Glauber, Phys. Rev. 131, 2766 (1963).  
<sup>5</sup>R. J. Glauber, in *Quantum Optics and Electronics, Les Houches Summer School* (Gordon and Breach, New York, 1964), p. 63.  
<sup>6</sup>See for example, J. P. Crutchfield, J. D. Farmer, and B. A. Huberman, Phys. Rev. 92, 45 (1982).  
<sup>7</sup>L. A. Orozco, A. T. Rosenberger, and H. J. Kimble, Phys. Rev. Lett. 53, 2547 (1984).  
<sup>8</sup>G. Broggi, E. Brun, B. Derighetti, P. F. Meier, M. Ravani, and R. Stoop, Technical Digest of the International Meeting on

Instabilities and Dynamics of Lasers and Nonlinear Optical Systems, Rochester, N.Y., 1985 (unpublished).

<sup>9</sup>J. L. Boulnois, A. van Lerberghe, P. Cottin, F. T. Arecchi, and G. P. Puccioni, Opt. Commun. 58, 124 (1986).  
<sup>10</sup>W. W. Chow, M. O. Scully, and E. W. Van Stryland, Opt. Commun. 15, 6 (1975).  
<sup>11</sup>L. A. Lugiato, L. M. Narducci, D. K. Bandy, and C. A. Pennise, Opt. Commun. 46, 64 (1983).  
<sup>12</sup>(a) D. K. Bandy, L. M. Narducci, C. A. Pennise, and L. A. Lugiato, in *Coherence and Quantum Optics V*, edited by L. Mandel and E. Wolf (Plenum, New York, 1984); (b) D. K. Bandy, L. M. Narducci, and L. A. Lugiato, J. Opt. Soc. Am. B 2, 148 (1985) and references quoted therein.  
<sup>13</sup>L. A. Lugiato, in *Progress in Optics*, edited by E. Wolf (North Holland, Amsterdam, 1984), Vol. XXI.  
<sup>14</sup>L. A. Lugiato, R. J. Horowicz, G. Strini, and L. M. Narducci, Phys. Rev. A 30, 1366 (1984).